PCP
PLANT & CELL PHYSIOLOGY

Regular Paper

ABA Regulates Subcellular Redistribution of OsABI-LIKE2, a Negative Regulator in ABA Signaling, to Control Root Architecture and Drought Resistance in *Oryza sativa*

Chengxiang Li[1], Hongyun Shen[1], Tao Wang[1,2] and Xuelu Wang[2,*]

[1]National Key Laboratory of Genetic Engineering, School of Life Sciences, Fudan University, Shanghai 200433, China
[2]National Key Laboratory of Crop Genetic Improvement, College of Life Science and Technology, Huazhong Agricultural University, Wuhan 430070, Hubei, China
*Corresponding author: E-mail, xlwang@mail.hzau.edu.cn; Fax, +86-27-87287366.
(Received January 7, 2015; Accepted October 13, 2015)

The phytohormone ABA is a key stress signal in plants. Although the identification of ABA receptors led to significant progress in understanding the Arabidopsis ABA signaling pathway, there are still many unsolved mysteries regarding ABA signaling in monocots, such as rice. Here, we report that a rice ortholog of *AtABI1* and *AtABI2*, named *OsABI-LIKE2* (*OsABIL2*), plays a negative role in rice ABA signaling. Overexpression of *OsABIL2* not only led to ABA insensitivity, but also significantly altered plant developmental phenotypes, including stomatal density and root architecture, which probably caused the hypersensitivity to drought stress. OsABIL2 interacts with OsPYL1, SAPK8 and SAPK10 both in vitro and in vivo, and the phosphatase activity of OsABIL2 was repressed by ABA-bound OsPYL1. However, unlike many other solely nuclear-localized clade A type 2C protein phosphatases (PP2Cs), OsABIL2 is localized in both the nucleus and cytosol. Furthermore, OsABIL2 interacts with and co-localized with OsPYL1 mainly in the cytosol, and ABA treatment regulates the nucleus–cytosol distribution of OsABIL2, suggesting a different mechanism for the activation of ABA signaling. Taken together, this study provides significant insights into rice ABA signaling and indicates the important role of *OsABIL2* in regulating root development.

Keywords: Keywords: ABA • Clade A type 2C protein phosphatase • Drought resistance • *Oryza sativa* • *OsABIL2* • Root architecture • Subcellular redistribution.

Abbreviations: BiFC, bimolecular fluorescence complementation; DJ, Dongjin; ER, endoplasmic reticulum; GFP, green fluorescent protein; GST, glutatione *S*-transferase; MBP, maltose-binding protein; MS, Murashige and Skoog; PHS, pre-harvest sprouting; PP2C, type 2C protein phosphatase; qRT-PCR, quantitative real-time PCR; SAPK, osmotic stress/ABA-activated protein kinase; SEM, scanning electron microscopy; SnRK2, SNF1-RELATED PROTEIN KINASE 2; YFP, yellow fluorescent protein.

Introduction

ABA plays important roles in responding to various stresses in many plant species. A core ABA signaling pathway has been established in Arabidopsis (Fujii et al. 2009). ABA is perceived by a class of soluble proteins named PYRABACTIN RESISTANCE1 (PYR1)/PYRABACTIN RESISTANCE1-LIKE (PYL)/REGULATORY COMPONENTS OF ABA RECEPTOR (RCAR) (Ma et al. 2009, Park et al. 2009). ABA binding promotes the interaction of ABA receptors with the clade A type 2C protein phosphatases (clade A PP2Cs), such as ABSCISIC ACID-INSENSITIVE 1 (ABI1) and ABSCISIC ACID-INSENSITIVE 2 (ABI2) (Leung et al. 1994, Meyer et al. 1994, Leung et al. 1997) to release their inhibition and dephosphorylation of the subclass III SNF1-RELATED PROTEIN KINASE 2 (SnRK2) family kinases, including SnRK2.2/2.3/2.6 (Mustilli et al. 2002, Fujii et al. 2007, Fujii et al. 2011, Fujita et al. 2009, Umezawa et al. 2009). The activated SnRK2s then phosphorylate and activate many downstream transcription factors (Kobayashi et al. 2005, Fujii et al. 2007), such as the ABA-responsive element-binding factors (ABFs) (Choi et al. 2000, Kang et al. 2002), to regulate the expression of thousands of genes.

In rice, aboitic stresses are major causes of yield loss (Mickelbart et al. 2015), and many studies on ABA signaling focus on ABA/stress-responsive transcription factors (Shinozaki and Yamaguchi-Shinozaki 2007, Todaka et al. 2012). However, study of upstream ABA signaling is very limited. It was reported that OsPYL/RCAR5 (Os05g12260), an AtPYR homolog in rice, functions as a positive regulator in rice ABA signaling (Kim et al. 2012). OsPYL/RCAR5 interacts with a clade A PP2C, OsPP2C30 (Os03g16170), and OsPP2C30 can interact with an SnRK2, SAPK2 (osmotic stress/ABA-activated protein kinase 2). In addition, SAPK2 can interact with an ABRE-binding transcription factor OREB1. Thus, OsPYL/RCAR5–OsPP2C30–SAPK2–OREB1 form a regulatory module in rice (Kim et al. 2012). In addition, another rice SnRK2, OSRK1 (also named osmotic stress/ABA-activated protein kinase 6, SAPK6), was shown to be dehydration inducible, and OSRK1 could phosphorylate OREB1 (Chae et al. 2007). SAPK2 is quite similar to SnRK2.7 and SnRK2.8 (belonging to the subclass II SnRK2s), while SAPK6 is similar to SnRK2.9 (belonging to the subclass I SnRK2s). However, unlike the well characterized ABA-responsive subclass III SnRK2s in Arabidopsis, the transcription and phosphorylation of SAPK2 are induced by

Plant Cell Physiol. 56(12): 2396–2408 (2015) doi:10.1093/pcp/pcv154, Advance Access publication on 21 October 2015, available online at www.pcp.oxfordjournals.org

osmotic stress but not by ABA (Kobayashi et al. 2004). On the other hand, it was recently reported that seven putative rice ABA receptors, OsPYL1, 2, 3, 6, 10, 11 and 12, can repress the protein phosphatase activity of some clade A PP2Cs in both an ABA-dependent and ABA-independent manner, and the crystal structure of the ABA–OsPYL2–OsPP2C09 (Os01g62760) complex has been determined (He et al. 2014).

Clade A PP2Cs are important components in the core ABA signaling pathway of Arabidopsis, but the function of the clade A PP2Cs in rice ABA signaling remains to be investigated. OsPP2C30 can interact with OsPYL/RCAR5 both in vivo and in vitro, and OsPYL/RCAR5 can interact with another rice clade A PP2C, OsPP2C49 (Os05g38290), in an ABA-dependent manner in yeast two-hybrid assays (Kim et al. 2012). In vitro experiments showed that another two clade A PP2Cs, OsPP2C06 (Os01g40094) and OsPP2C09 (Os01g62760), are targets of putative rice ABA receptors (He et al. 2014). Recently, another ABA-inducible clade A PP2C gene, *OsPP108* (*Os09g15670*), was reported. Overexpression of *OsPP108* enhanced rice salt and drought resistance but caused ABA insensitivity in Arabidopsis (Singh et al. 2015).

To date, all the reported rice clade A PP2Cs have been found to be localized in the nucleus (Kim et al. 2012, Li et al. 2013, Singh et al. 2015), but the subcellular localization of rice clade A PP2Cs in ABA signaling has not been reported. In Arabidopsis, the nuclear localization of ABI1 is critical for its function (Moes et al. 2008). In addition, although a relatively conserved ABA early signaling pathway in rice was proposed, the physiological functions and the regulation mechanisms of many ABA signaling components in rice are poorly understood. In this study, we functionally characterized a new rice clade A PP2C member, OsABIL2, which negatively regulates ABA signaling and affects both drought resistance and root architecture. Interestingly, its subcellular localization was found to be regulated by ABA. Our study provides insight into the ABA signaling mediated by OsABIL2, and its role in rice development and abiotic stress responses.

Results

OsABIL2 is homologous to AtABI1/AtABI2

In order to investigate the function of rice clade A PP2Cs, we constructed a phylogenetic tree with clade A PP2Cs from rice and Arabidopsis (**Supplementary Fig. S1**). Based on their sequence similarity and bootstrap values, these PP2Cs were further classified into four subgroups, named A-I to A-IV. The A-I subgroup contains three rice members and four Arabidopsis members including *ABI1* and *ABI2*. Therefore, we named the three rice PP2C genes *OsABI-LIKE1* (*OsABIL1*, *Os01g40094*), *OsABI-LIKE2* (*OsABIL2*, *Os05g51510*) and *OsABI-LIKE3* (*OsABIL3*, *Os05g46040*). Among them, *OsABIL2* and *OsABIL1* are the closest homologs of *AtABI1* and *AtABI2*.

OsABIL2 is mainly expressed in leaf blades and sheaths, and may not be transcriptionally feedback regulated by ABA

We used quantitative real-time PCR (qRT-PCR) to demonstrate the expression profile of *OsABIL2* and the other nine rice clade A PP2C genes in different tissues. *OsABIL1* was broadly expressed in most tissues (**Supplementary Fig. S2**), and *OsABIL2* was mainly expressed in leaf blades and sheaths of seedlings and adult plants (**Fig. 1A, B**). The expression of most PP2Cs was relatively low in reproductive tissues as compared with that in vegetative tissues (**Supplementary Fig. S2**).

On the other hand, the negative feedback of ABA signaling was observed by ABA-induced expression of *AtABI1* and *AtABI2* (Merlot et al. 2001). Thus, we measured the expression of *OsABIL2* and the other clade A PP2C genes after ABA treatment and found that, with the exception of *OsABIL2*, all of the other PP2C genes were highly induced by ABA (**Fig. 1C**). Moreover, the different subgroup members behaved slightly differently in ABA responses: the A-I and A-II subgroups showed relatively slight but consistent ABA induction, while the A-III and A-IV subgroups showed a dramatic ABA induction at the early stage, but the fold induction was decreased after 3 h (**Fig. 1C**). These features suggested diverse regulatory methods. Therefore, unlike other clade A PP2C genes, *OsABIL2* may not be greatly involved in the negative feedback regulation by ABA at the transcription level, suggesting a possible unknown regulatory mechanism of *OsABIL2*.

OsABIL2 overexpression led to pre-harvest sprouting and ABA insensitivity in rice

To investigate further the biological function of clade A PP2Cs in rice, we generated the overexpression lines of *OsABIL1* and *OsABIL2*. We found that the *OsABIL1* overexpression (*OsABIL1-ox*) seedlings (T_0 generation) were rapidly dehydrated (**Supplementary Fig. S3D**), and most of them were dead when transplanted to soil. The survivors exhibited dramatically reduced fertility and severe pre-harvest sprouting (PHS), so we could study these materials further (**Supplementary Fig. S3A–C**). The *OsABIL2* overexpression lines showed about a 20- to 160-fold overexpression in the T_0 generation (**Supplementary Fig. S4**). Similar to *OsABIL1-ox* lines, most of the *OsABIL2* overexpression lines struggled to survive and had a poor fertility, so we used two lines (*OsABIL2-ox-4* and *OsABIL2-ox-6*) with moderately altered phenotype and reasonable fertility for further study. These lines showed a significant PHS phenotype in the paddy field, with about 30% of grains germinated on the panicles, as compared with only 0.75% in the wild type (**Fig. 2A**), suggesting that *OsABIL2* inhibits ABA signaling to reduce seed dormancy.

To investigate further the role of *OsABIL2* in rice ABA signaling in planta, we checked the sensitivity of *OsABIL2* overexpression lines to ABA in multiple respects. We found that the induction of ABA-up-regulated genes, including *RAB21*,

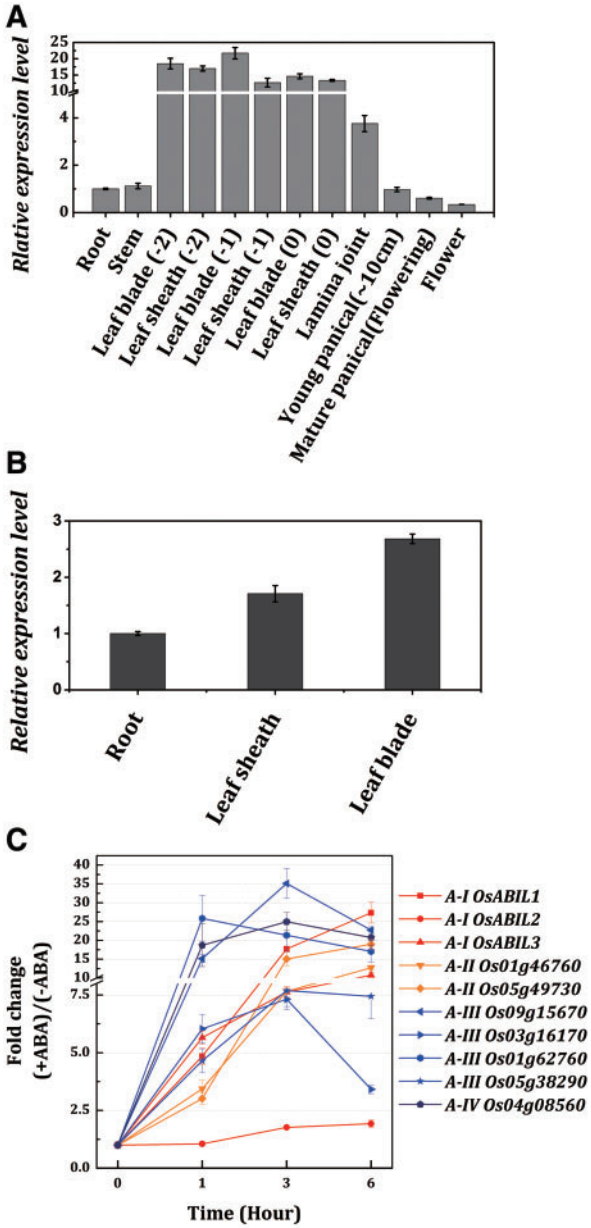

Fig. 1 The expression pattern of OsABIL2 and the ABA induction of rice clade A PP2Cs. (A) The expression pattern of *OsABIL2* in various tissues at the rice heading stage. Root samples were collected from field-grown rice. Stems were from the first internode below the panicles. Leaf (0) indicates the flag leaf. Leaf (−1) indicates the leaf below the flag leaf. Leaf (−2) indicates the leaf below leaf (−1). The lamina joints were from flag leaves. The young panicle is a panicle before head sprouting of about 10 cm in length. The mature panicle indicates a panicle during flowering. The relative expression levels of different tissues are normalized to the expression in root. Data are means ± SD. (B) The expression pattern of *OsABIL2* in 1-week-old seedlings. The relative expression levels of different tissues are normalized to the expression in root. Data are means ± SD. (C) ABA induced the expression of rice clade A PP2Cs. The fold change showed the relative expression ratio of ABA treatment/mock treatment at the indicated time point. Data are means ± SD. The A-I to A-IV groups refer to **Supplementary Fig. S1**. The A-I group members are shown with red lines; the A-II group members are shown with orange lines; the A-III group members are shown with blue lines; and the A-IV group members are shown with dark blue lines.

OsRD22, *OsLEA3*, *BZ8*, *TRAB1*, *OsNCED4* and *OsZEP1*, was dramatically reduced in the *OsABIL2* overexpression lines compared with the wild type Dongjin (DJ) (**Fig. 2B**). Moreover, the germination rate of the *OsABIL2* overexpression lines was much higher than that of the wild type in half-strength Murashige and Skoog (1/2 MS) medium containing 1 μM ABA (**Fig. 2C**), indicating that the *OsABIL2* overexpression lines were less sensitive to ABA than the wild type. In addition, it is well known that ABA can repress plant growth, so we measured plant height after long-term ABA treatment. We found that 2 μM ABA can strongly inhibit shoot growth of the wild type, but not that of *OsABIL2-ox-4* and *OsABIL2-ox-6* (**Fig. 2D**). Taking these findings together, we concluded that *OsABIL2* is a critical negative regulator in rice ABA signaling.

Overexpression of *OsABIL2* enhanced water loss and affected root architecture.

Because ABA plays a critical role in abiotic stress resistance, we attempted to explore the biological role of *OsABIL2* in rice drought responses. We tested the drought resistance of 4-week-old seedlings of *OsABIL2-ox-4*, and found that it was hypersensitive to drought as compared with the wild type (**Fig. 3A**). In particular, the water loss rate of the *OsABIL2-ox-4* excised leaves was significantly higher than that of the wild type (**Fig. 3B**). Using scanning electron microscopy (SEM), we observed that there were more stomata (about 50% more than in the wild type per unit area) on the abaxial side (**Fig. 3C–F**) of rice leaves. However, we could not clearly observe the stomatal aperture probably due to technical limitations. A previous study in Arabidopsis indicated that ABA can affect stomatal density by inhibiting stomatal initiation (Tanaka et al. 2013), suggesting that ABA might also regulate stomatal patterning in rice.

Furthermore, we carefully observed the root architecture of *OsABIL2-ox-4* and found that it had shortened seminal and crown roots, reduced root diameter and reduced total root number as compared with the wild type (**Fig. 3G**). We also found that the young crown roots of *OsABIL2-ox-4* had shorter and fewer root hairs (**Fig. 3H**), and the lateral root number was also decreased (**Fig. 3I**). Because ABA can induce root hair elongation and root tip swelling in rice (Chen et al. 2006), we then tested root hair induction triggered by ABA. We found that both the wild type and *OsABIL2-ox-4* grew few root hairs in water. However, when the 3-day-old water-grown seedlings were moved into solution containing different concentrations of ABA for 36 h, the root hair induction of the wild type was observed in solution containing ≥1 μM ABA, and root tip swelling was observed in ≥2 μM ABA. In contrast, root hair induction of *OsABIL2-ox-4* was observed until the ABA concentration was as high as 10 μM (**Fig. 3J, K**), indicating that overexpression of *OsABIL2* led to significant insensitivity of root hair induction to ABA. Therefore, the weakened root system of the *OsABIL2* line may lead to a greatly decreased water uptake and hypersensitivity to drought.

We also investigated the phenotypes of loss-of-function lines. In this study, we ordered some T-DNA lines of

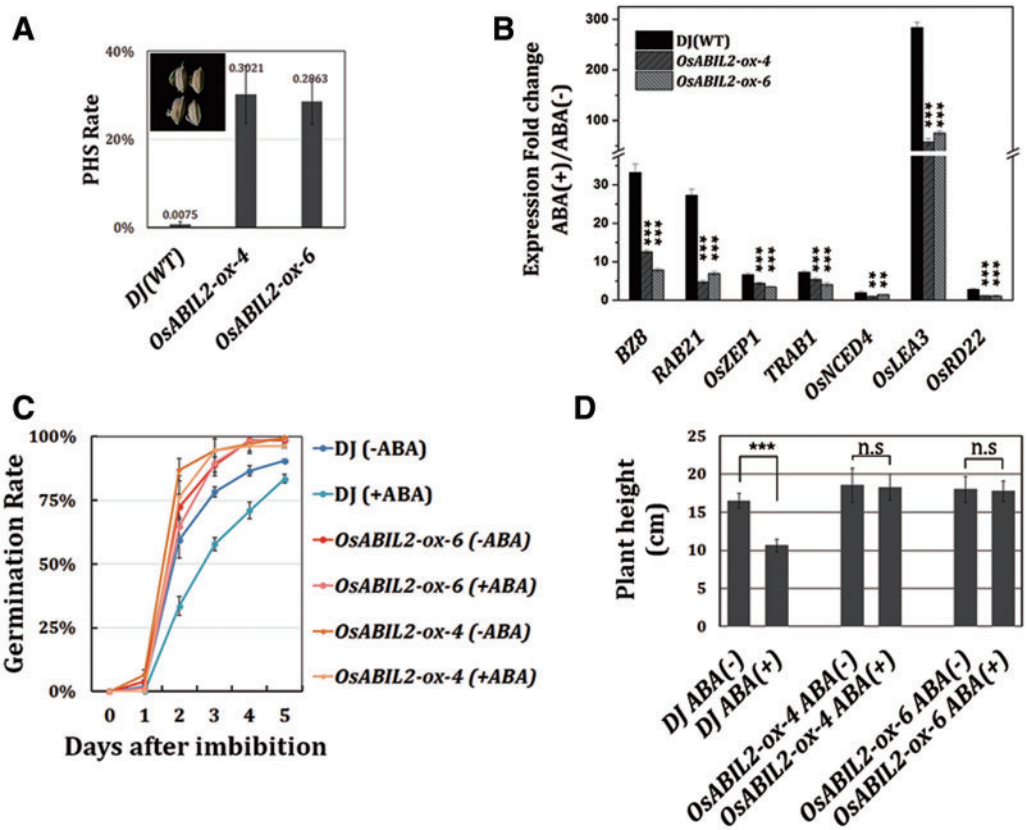

Fig. 2 *OsABIL2* overexpression causes pre-harvest sprouting (PHS) and ABA insensitivity. (A) The PHS rate of DJ and the *OsABIL2* overexpression lines. Photographs show typical PHS grains from a field-grown plant. Data are means ± SD. (B) Marker gene induction in the *OsABIL2* lines was hyposensitive to ABA The fold changes after 50 μM ABA treatments are represented. (C) Seed germination of the *OsABIL2* lines was insensitive to ABA . In the (−ABA) group samples, surface-sterilized seeds were plated on 1/2 MS, and in the (+ABA) group samples, surface-sterilized seeds were planted on 1/2 MS with 1 μM ABA. (D) The *OsABIL2* lines were insensitive to ABA in terms of above-ground tissue growth inhibition. Sixteen seedlings of each treatment were measured. In the (−ABA) group, seedlings were grown in water and, in the ABA (+) group, seedlings were grown in water with 2 μM ABA. Error bars indicate the SD. ***$P < 0.001$; **$P < 0.01$; n.s., not significant.

OsABIL1 and *OsABIL2* (Jeon et al. 2000, Jeong et al. 2006). The *OsABIL1* expression in *osabil1* (*PFG_1A-08436*) was <1% of that of the wild type DJ, and the *OsABIL2* expression level in *osabil2* (*PFG_2B-60103*) was reduced to about 50% of that of the wild type Hwayoung (HY) (**Supplementary Fig. S5A–C**). However, we found that *osabil1* and *osabil2* exhibited ABA sensitivity similar to that of the wild type DJ and HY in root hair induction and growth repression of the above-ground tissues (**Supplementary Fig. S5D, E**). It may result from gene redundancy, because the sequences of the proteins encoded by *OsABIL1*, *OsABIL2* and *OsABIL3* are highly conserved (**Supplementary Fig. S1**). In Arabidopsis, only multiple knock-out of clade A PP2Cs can lead to ABA hypersensitivity (Saez et al. 2006, Rubio et al. 2009), supporting the redundancy of clade A PP2Cs in ABA signaling.

OsABIL2 interacts with the putative ABA receptor OsPYL1 and the downstream components SAPK8 and SAPK10.

In order to establish an OsABIL2-mediated ABA signaling pathway in rice, we searched the rice homologs of *AtSnRK2.2/2.3/2.6* and *AtPYR*. Based on sequence analysis, rice *SAPK8*, *SAPK9* and *SAPK10* are highly similar to the subclass III SnRK2s in Arabidopsis (**Supplementary Fig. S6B**). In addition, it was reported that SAPK10 can phosphorylate TRAB1, an ABA-responsive bZIP transcription factor in rice (Kagaya et al. 2002, Kobayashi et al. 2005). Therefore, we speculated that SAPK8/9/10 might be key components in rice ABA signaling, and thus we used two of them, SAPK8 and SAPK10, for further study. We found that, of these, *OsPYL1* (*Os10g42280*) (He et al. 2014) is the one with the highest sequence similarity (49.5% identity) to *AtPYR*; therefore, we chose it for further study (**Supplementary Fig. S6A**).

Our bimolecular fluorescence complementation (BiFC) assays indicated that OsABIL2 can interact with OsPYL1, SAPK8 and SAPK10 in *Nicotiana benthamiana* pavement cells. Interestingly, the BiFC signal of the OsABIL2–OsPYL1 interaction showed a 'ring shape' around the nucleus, while the BiFC signal of OsABIL2–SAPK8/10 interactions was detected in both the nucleus and cytosol (**Fig. 4A**), suggesting their subcellular localization may be regulated by an unknown mechanism. We further used yeast two-hybrid and in vitro pull-down assays, and demonstrated that the direct interaction between OsPYL1 and OsABIL2 is ABA dependent (**Fig. 4B, C**).

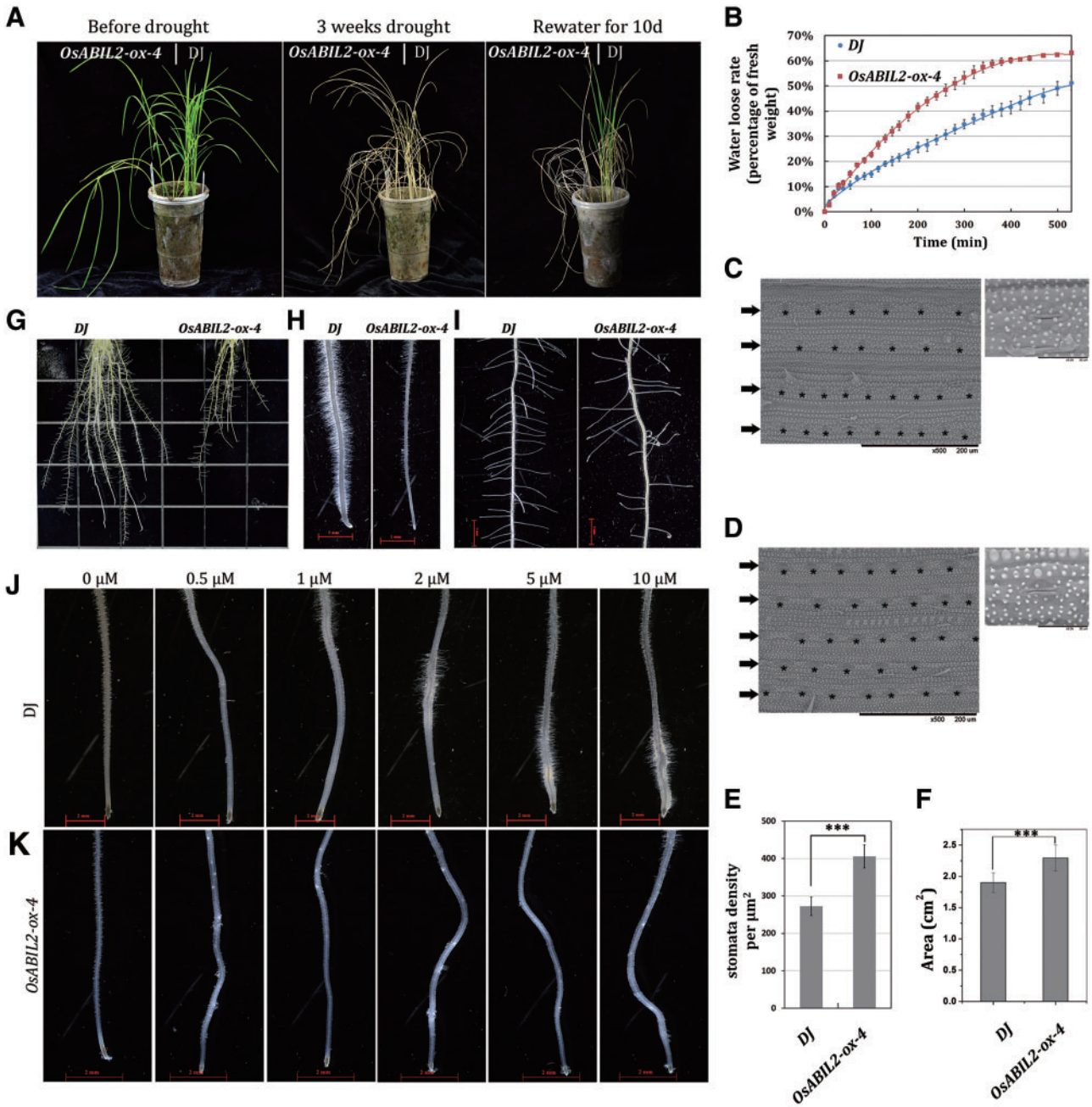

Fig. 3 Rapid water loss and a weak root system lead to drought hypersensitivity of the *OsABIL2* overexpression (*OsABIL2-ox*) plants. (A) The *OsABIL2-ox* line was hypersensitive to drought. Left: the *OsABIL-ox* line; right, the wild type DJ. (B) Kinetics of water loss of the excised leaves. (C) The adaxial surface of a typical DJ leaf. The left panel shows the leaf adaxial surface. Black arrows indicate stomatal arrays. Asterisks indicate individual stomata. The right panel shows a close-up view of an individual stoma. (D) The adaxial surface of the *OsABIL2-ox* leaf. The left panel shows the leaf adaxial surface. Black arrows indicate stomatal arrays. Asterisks indicate individual stomata. The right panel shows a close-up view of an individual stoma. (E) Stomatal density of DJ and *OsABIL2-ox*. (F) Leaf area of DJ and *OsABIL2-ox*. (G) Root architecture of seedlings grown on 1/2 MS medium. Left, DJ; right, the *OsABIL2-ox* line. (H) Close-up view of crown root tips of DJ (left) and the *OsABIL2-ox* line (right). (I) Close-up view of lateral roots of DJ (left) and the *OsABIL2-ox* line (right). (J) Responses of root tip growth of DJ to ABA. Scale bars = 2 mm. (K) Responses of the root tip growth of *OsABIL2-ox-4* to ABA. Scale bars = 2 mm. Data are means ± SD. ***$P < 0.001$.

Moreover using a semi-in vivo pull-down assay, we also found that additional ABA enhanced the physical interaction of OsABIL2 with OsPYL1 (**Fig. 4D**). In Arabidopsis, the ABA receptor binding to clade A PP2Cs cannot weaken the interactions between clade A PP2Cs and SnRK2s (Nishimura et al. 2009, Umezawa et al. 2009). In our study, the interaction between OsABIL2 and SAPK8/10 was also detected by semi-in vivo pull-down assay (**Fig. 4E**). Interestingly, the addition of ABA and/or OsPYL1 to plant extract of the *OsABIL2* overexpression line can clearly weaken the interaction between SAPK10/SAPK8 and OsABIL2 (**Fig. 4E**). However, when using an in vitro pull-down assay to test their competition, OsPYL1 only has a weak ability to

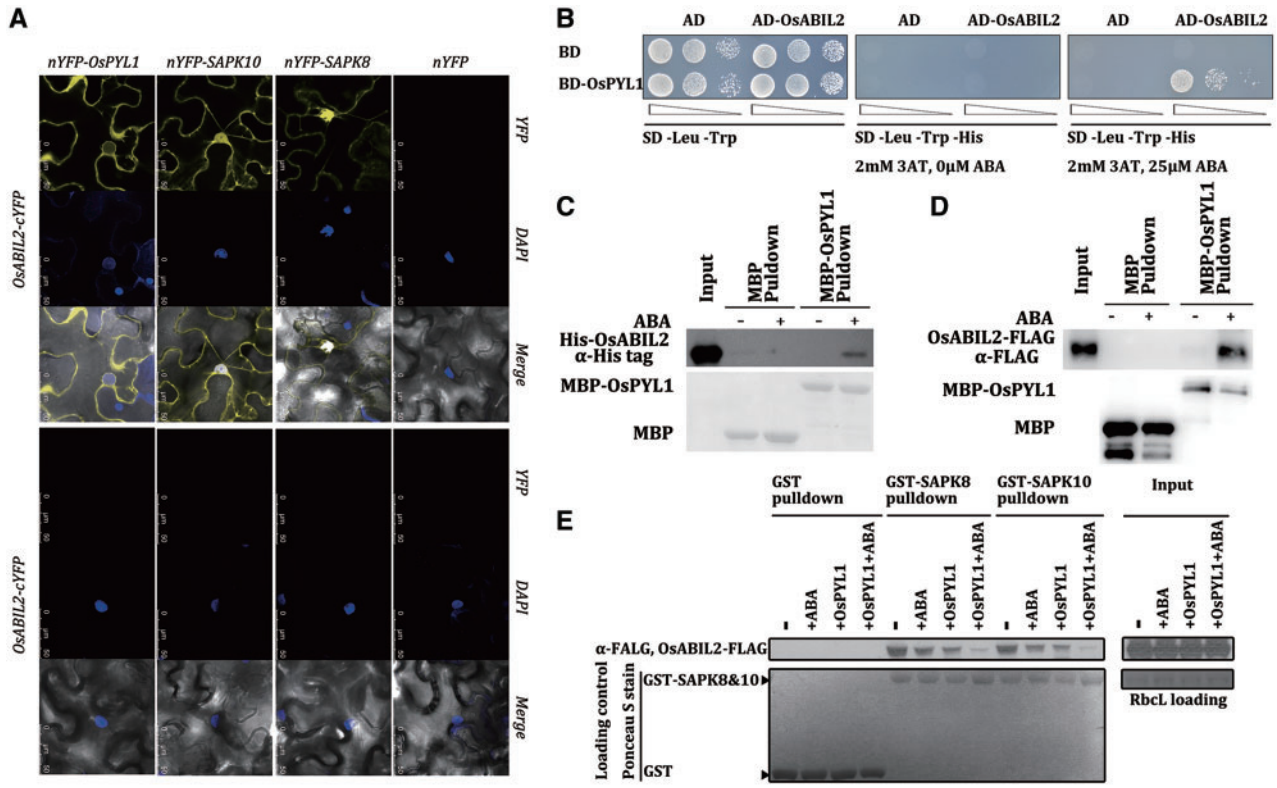

Fig. 4 OsABIL2 interacts with OsPYL1, SAPK10 and SAPK8. (A) OsABIL2 interacts with OsPYL1, SAPK10 and SAPK8 in BiFC assays. The N-YFP and C-YFP constructs that were used in each combination are presented at the top and left side. Scale bar = 50 μm. (B) OsABIL2 interacts with OsPYL1 in an ABA-dependent manner in yeast two-hybrid assays. OsABIL2 was fused to the activation domain (AD) and OPYL1 to the binding domain (BD). ABA was added in the culture medium. (C) OsABIL2 interacts with OsPYL1 in an ABA-dependent manner in the in vitro pull-down assays. MBP and MBP–OsPYL1 were used as bait and the loading amounts are shown in the bottom panel. Pull-downed His-OsABIL2 is shown in the upper panel. (D) OsABIL2 interacts with OsPYL1 in an ABA-dependent manner in the semi-in vivo pull-down assays. MBP and MBP–OsPYL1 were used as bait and the loading amounts are shown in the bottom panel. Pull-downed OsABIL2-FLAG is shown in the upper panel. (E) ABA-bound OsPYL1 inhibits the interaction of OsABIL2 with SAPK10 and SAPK8 in the semi-in vivo pull-down assays. GST–SAPK8 and GST–SAPK10 were used as bait, and the loading controls are shown on the left part of the bottom panel (Ponceau S staining). The total protein extract from the *OsABIL2* overexpression line was divided equally into 12 parts and used as prey. ABA and/or MBP–OsPYL1 were added in the pull-down mixture and incubated with bead-bound bait and the rice protein extract. OsABIL2-FLAG was detected by anti-FLAG antibody. The Ponceau S-stained Rubisco large subunit (RbcL) was used as a loading control.

compete SAPK10 away from OsABIL2 (**Supplementary Fig. S7**), as compared with that in the semi-in vivo assay. Therefore, we proposed that some other unknown components in vivo might help ABA bind to OsPYL1 to trigger release of SnRK2s.

OsABIL2 can dephosphorylate SAPK8 and SAPK10, which can be repressed by ABA-bound OsPYL1

Because phosphorylation of subclass III SnRK2s is essential for ABA signaling in Arabidopsis (Fujii and Zhu 2009, Fujita et al. 2009, Fujii et al. 2011, P. Wang et al. 2013, Cai et al. 2014), we tested whether the phosphorylation of SAPK10 and SAPK8 is regulated by OsABIL2. Similar to their Arabidopsis homologs, the autophosphorylation of SAPK10 and SAPK8 can be detected by Phos-Tag marked SDS–PAGE (**Fig. 5**). In addition, we found that OsABIL2 can significantly dephosphorylate SAPK8 and SAPK10 in vitro, and the ABA-bound OsPYL1 can significantly inhibit its effect on the dephosphorylation of SAPK8 and SAPK10 (**Fig. 5**). Therefore, we propose that OsPYL1–OsABIL2–SAPK8/10 can form an upstream ABA signaling module in rice.

The subcellular localization of OsABIL2 is regulated by OsPYL1 and ABA

As the BiFC signals of the OsABIL2–OsPYL1 and OsABIL2–SAPK10/8 interactions showed clearly different features (**Fig. 3A**), we then explored the subcellular localization of *OsABIL2* and its regulation. Interestingly, we found that, in *N. benthamiana* pavement cells, OsABIL1–mCherry was mainly localized in the nucleus with a weak cytosolic signal (**Fig. 6A**), but a significant amount of OsABIL2–mCherry was found in the cytosol (**Fig. 6B**), which was clearly different from OsABIL1, and the previously reported OsPP2C30, OsSIPP2C1 and OsPP108. On the other hand, OsPYL1–green fluorescent protein (GFP), SAPK10–GFP and SAPK8–GFP are all localized in both the nucleus and cytosol in *N. benthamiana* pavement cells (**Fig. 6C–E**), and OsPYL1 and OsABIL2 were mostly co-localized in the cytosol and formed a 'ring shape' around the

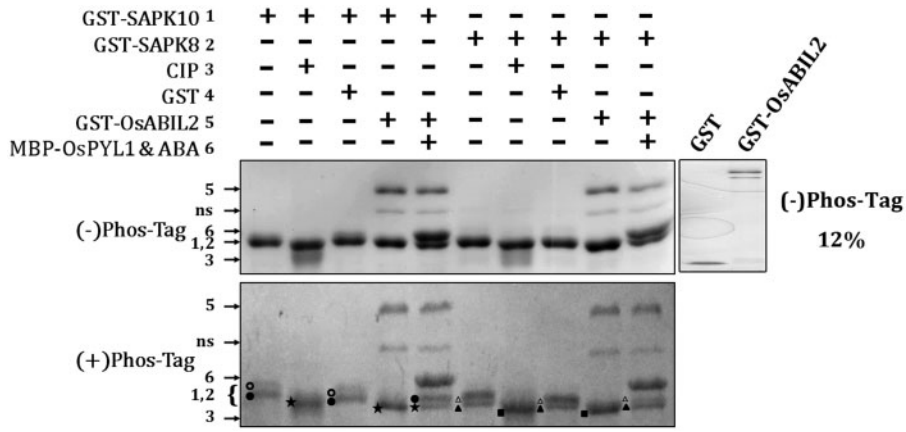

Fig. 5 OsABIL2 dephosphorylates SAPK10 and SAPK8, and OsPYL1 inhibits the phosphatase activity of OsABIL2. The phosphorylated SAPK10 is marked with filled circles, and the hyperphosphorylated SAPK10 is marked with open circles. The phosphorylated SAPK8 is marked with filled triangles, and the hyperphosphorylated SAPK8 is marked with open triangles. CIP (calf intestinal alkaline phosphatase) can dephosphorylate SAPK10 and SAPK8; the dephosphorylated SAPK10 is marked with stars, and the dephosphorylated SAPK8 is marked with filled squares. Other components in the reaction system are shown with corresponding numbers, and 'ns' indicates a non-specific band. OsABIL2 can effectively dephosphorylate SAPK10 and SAPK8, which was inhibited by ABA-bound OsPYL1. The Phos-Tag gel (8%) containing 25 μM Phos-Tag with 100 μM $MnCl_2$ shows the phosphorylation status, and the normal gel (8%) shows the loading amount of all the components. GST and GST–OsABIL2 were visualized using another gel (12%). All bands were visualized by Coomassie Brilliant Blue (CBB) staining.

nucleus (**Fig. 6F**), which was consistent with the BiFC signal (**Fig. 3A**). Moreover co-expression with OsPYL1–GFP weakened the nuclear localization of OsABIL2–mCherry (**Fig. 6F, B**). In contrast, OsABIL2 was co-localized with SAPK8 and SAPK10 in both the nucleus and the cytosol (**Fig. 6G, H**), and formed a 'stuffed nucleus'. As the level of transiently expressed protein is not stable and homogeneous, we used a stable *OsABIL2* overexpression rice line to prepare protoplasts to monitor the OsABIL2-FLAG subcellular distribution by transiently expressing OsPYL1 with ABA treatment. We detected the FLAG-tag protein levels in each fraction by Western blotting. β-Tublin was used as the loading control for the total protein and cytosol fractions. We found that when we expressed OsPYL1 in tobacco leaves with additional ABA, the nuclear localized OsABIL2-FLAG was reduced and the cytosolic fraction was increased (**Fig. 6I**). We further compared the protein levels of OsABIL2-FLAG in the nucleus and cytosol fraction before and after ABA treatment in rice seedlings, and found that ABA treatment reduced the nuclear localization and enhanced the cytosolic localization of OsABIL2-FLAG (**Fig. 6J**). As the interaction of OsABIL2 and OsPYL1 depends on ABA, the ABA-regulated subcellular localization of OsABIL2 may be a different regulatory mechanism in the rice ABA signaling pathway.

Because the signal of OsPYL1 and OsABIL2 co-localization and interaction formed a 'ring shape' around the nucleus, which is probably a feature of the endoplasmic reticulum (ER), we tested their co-localization with an ER marker in tobacco. We found that the co-localization signal of OsPYL1 with OsABIL2 around the nucleus was merged with ER–cyan fluorescent protein (CFP) (**Fig. 7A**). On the other hand, the ER marker showed a typically reticular appearance in the cytosol; however, neither OsABIL2–mCherry nor OsPYL1–GFP showed this feature (**Fig. 7B**). Similarly, the BiFC signal of OsPYL1–OsABIL2 interaction was partially co-localized with ER–mCherry around the nucleus (**Fig. 7C**), but poorly co-localized with reticular ER in the cytosol (**Fig. 7D, E**).

Discussion

In this study, we demonstrated that OsPYL1–OsABIL2–SAPK8/10 together form a dynamic module initially to transduce ABA signaling in rice, which exhibited some unique features different from the previously reported rice ABA regulatory module OsPYL/RCAR5–OsPP2C30–SAPK2 and the ABA module in Arabidopsis. Our results suggested that the cytosol–nucleus redistribution of OsABIL2 may be a novel regulatory mechanism compared with its homologs mainly localized in the nucleus. To date, AtABI1 (Moes et al. 2008), OsPP2C30 (Kim et al. 2012), OsSIPP2C1 (Li et al. 2013), OsPP108 (Singh et al. 2015) and OsABIL1 (**Fig. 6A**) were found localized predominantly in the nucleus. However, OsABIL2 localized in both the cytosol and nucleus, and its subcellular localization was regulated by OsPYL1 and ABA. One possibility is that, at the basal ABA level, OsABIL2 interacts with SAPK8/10 and represses their kinase activity in the nucleus, whereas when ABA increased, ABA-bound receptors such as OsPYL1 can compete SAPK8/10 away and bind to OsABIL2 in the cytosol, which further reduces OsABIL2 in the nucleus. Thus, the activities of SAPK8/10 are released (**Supplementary Fig. S8**). In Arabidopsis, clade A PP2Cs continue to interact with SnRK2s even when they are bound by ABA receptors, so the subcellular localization of PP2Cs might not be regulated. In contrast, we find that OsPYL1 can reduce the interactions between OsABIL2 and SAPK8/10 in vivo, and a relatively weak competition can also be observed in vitro. Therefore, we proposed that in spite of the stable interactions between OsABIL2 and SAPKs, OsPYL1 can compete with SAPK8/10 on binding to OsABIL2 with the help

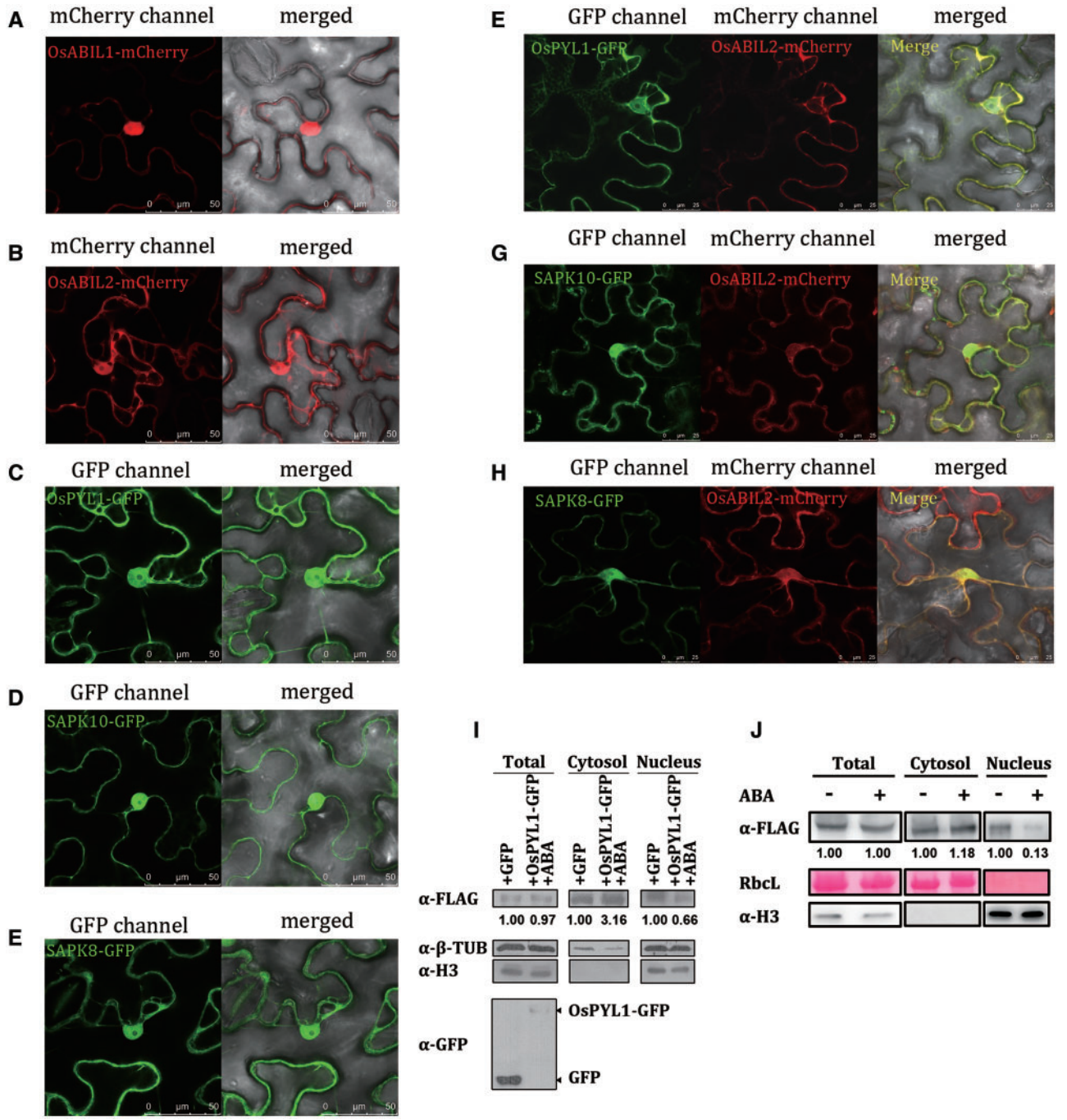

Fig. 6 Subcellular localization and co-localization analysis of OsABIL1, OsABIL2, OsPYL1, SAPK10 and SAPK8. (A) Subcellular localization of OsABIL1–mCherry. (B) Subcellular localization of OsABIL2–mCherry. (C) Subcellular localization of OsPYL1–GFP. (D) Subcellular localization of SAPK10–GFP. (E) Subcellular localization of SAPK8–GFP. Scale bar = 50 μm in (A–E). (F) Co-localization of OsABIL2–mCherry and OsPYL1–GFP. (G) Co-localization of OsABIL2–mCherry and SAPK10–GFP. (H) Co-localization of OsABIL2–mCherry and SAPK8–GFP. Scale bar = 25 μm in (F–H). (I) Immunoblot analysis of OsABIL2-FLAG in the total protein, cytosolic and nuclear fractions with or without addition of ABA-bound OsPYL1. Rice protoplasts from *OsABIL-ox-4* seedlings were transformed with *OsPYL1-GFP* and *GFP*, and then treated with or without 100 μM ABA for 2 h before cell fractionation. Histone H3 was used as a control of the nuclear fraction. β-Tubulin was used as a loading control for all of the fractions. Anti-GFP was used to detect the transiently expressed GFP and OsPYL1–GFP. The values below the anti-FLAG panel indicate the relative band intensities of the OsABIL2-FLAG that were normalized with anti-β-tubulin (J) Immunoblot analysis of OsABIL2-FLAG in the nuclear and cytosolic fractions with or without ABA treatments. The *OsABIL2-ox-4* seedlings were transplanted in solution with or without 5 μM ABA for 24 h. Histone H3 was used as loading control for the nucler fraction. The Ponceau S-stained Rubisco large subunit (RbcL) was used as a loading control. For the total protein and the cytosolic fractions, the values below the anti-FLAG panel indicate the relative band intensities of OsABIL2-FLAG that were normalized with RbcL. For the nuclear fractions, the values below the anti-FLAG panel indicate the relative band intensities of OsABIL2-FLAG that were normalized by anti H3.

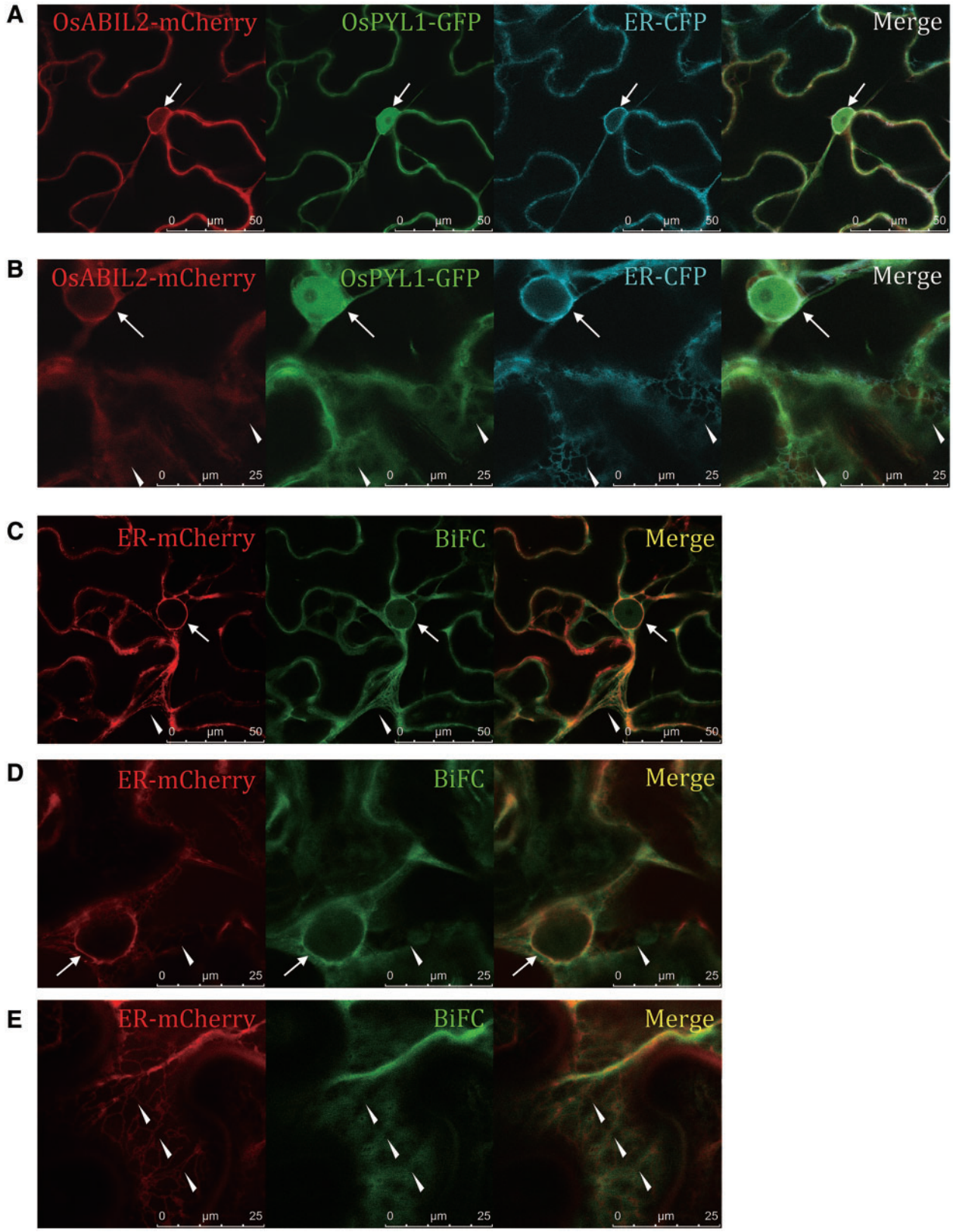

Fig. 7 Co-locolizatiom analysis of OsABIL2 and OsPYL1 with an ER marker. (A and B) Co-localization of OsABIL2–mCherry, OsPYL1 and ER–CFP. (A) General view of the co-localization in the whole cell. (B) Close-up view of the co-localization in the region surrounding the nucleus. Arrows show the 'ring shape' around the nucleus. Triangles show the reticular ER. (C–E) Co-localization of ER–mCherry and the BiFC signal of the OsPYL1–OsABIL2 interaction. (C) General view of the BiFC signal and ER in the whole cell. (D) Close-up view of the BiFC signal and ER in the region surrounding the nucleus. (E) Close-up view of the BiFC signal and ER in the reticular region. Arrows show the 'ring shape' around the nucleus. Triangles show the reticular ER. (A, C) Scale bar = 50 μm. (B, D, E) Scale bar = 25 μm.

of some other components in vivo. Our data provided evidence that ABA and OsPYL1 can regulate the subcellular localization of OsABIL2 by as yet unknown mechanisms. Considering that *OsABIL2* is not feedback regulated at the transcriptional level, the dynamic subcellular distribution of OsABIL2 may be a crucial regulatory mechanism for OsABIL2-mediated ABA signaling. However, it is still a mystery why both OsPYL1 and OsABIL2 could be localized in the nucleus, whereas OsPYL1–OsABIL2 is mainly localized in the cytosol; therefore, some other unknown components may be involved in regulating the subcellular distribution of OsABIL2.

On the other hand, we found that *OsABIL2* plays an important role in regulating root development. In Arabidopsis, it is well known that an enhanced water loss rate causes drought hypersensitivity of the *abi1-1* and *abi2-1* mutants, but the importance of an altered root development has not been explored (Leung et al. 1994, Meyer et al. 1994, Leung et al. 1997). The significant changes in root development and drought resistance of the *OsABIL2* line suggested that the root architecture may play an important role in drought resistance. Recently, it was reported that ABA or salt stress represses root growth by maintaining lateral root tip quiescence, which could be prevented by *abi1-1* expressed in the endodermis (Duan et al. 2013), suggesting that PP2Cs are involved in regulating root growth. However, *OsABIL2* overexpression inhibited ABA signaling but led to short roots in rice, which is inconsistent with the observation that ABA represses primary root growth in Arabidopsis. In fact, it was reported that ABA is needed for root elongation at low water potential in maize (Saab et al. 1990), and ABA is necessary for growth recovery under stress in Arabidopsis (Geng et al. 2013). Furthermore, a low concentration of polyethylene glycol (PEG) could promote root elongation, probably depending on ABA in both rice and Arabidopsis (Xu et al. 2013). In addition, ABA could promote root elongation in the *HAB1-ox* line, which is hyposensitive to ABA (Antoni et al. 2013). Therefore, it is likely that low concentrations of ABA promote root elongation, but high concentrations of ABA repress root growth. Thus, the short primary root of the *OsABIL2* line may have resulted from a severely reduced ABA signal. On the other hand, it was reported that the lateral root tips in Arabidopsis are more sensitive to ABA than the primary root tips (Duan et al. 2013). The longer lateral root observed in the *OsABIL2* overexpression line indicated that the ABA signaling output in the *OsABIL2* line may be sufficient for lateral root growth rather than primary root growth (**Fig. 3I**). Taken together, the *OsABIL2* overexpression line had shorter primary and crown roots and root hairs, and significantly impaired ABA-induced root hair elongation, which could dramatically reduce the water uptake.

With regard to above-ground tissues, similar to the gain-of-function mutants *abi1-1* and *abi2-1*, the *OsABIL2* overexpression line had an enhanced water loss rate, which might be caused by an increased number of stomata, although it is still unknown how OsABIL2 regulates stomatal development. Because rice leaves are thick with a high content of silicon, we had difficulty observing stomatal aperture. It was reported that the ABA-deficient mutant *aba2-1* had an increased stomatal number, while the ABA-accumulating double mutant *cyp707a1cyp707a3* had a decreased stomatal number in Arabidopsis (Tanaka et al. 2013). Therefore, we believe that ABA, or OsABIL2, has a potential role in regulating rice stomatal density. Apparently, the altered above-ground and under-ground organ development together lead to high drought sensitivity of *OsABIL2* overexpression lines.

Our current data and previous discoveries suggested a novel model for the OsABIL2-mediated ABA signaling in rice (**Supplementary Fig. S8**). In the basal state, OsABIL2 interacts with SAPK8 and SAPK10 to repress their activity. With ABA binding, OsPYL1 can interact with OsABIL2, which in turn causes a subcellular redistribution of OsABIL2 in the cytosol and releases the inhibition on SAPK8/10 in the nucleus. Then the phosphorylated SAPK8/10 can activate downstream transcription factors to regulate ABA-responsive gene expression to respond to environmental cues and regulate plant development. In the future, it will be interesting to investigate the underlying molecular mechanism by which OsABIL2 or ABA signaling regulates stomatal and root development in plants.

Materials and Methods

Plant materials and growth conditions

The wild-type rice DJ (*O. sativa* L. cv. *japonica*) and HW (*O. sativa* L. cv. *japonica*) were used in this work. The *OsABIL2* and *OsABIL1* overexpression lines and *osabil1* (T-DNA line, *PFG_1A-08436*) were in the DJ background, and *osabil2* (T-DNA line, *PFG_2B-60103*) was in the HW background. The T-DNA lines were obtained from Professor Gynheung An, Kyung Hee University, Republic of Korea. The primers used for genotyping are listed in **Supplementary Table S1**.

For physiological analysis, the rice seeds were imbibed for 2 d at 30°C, and the germinated seeds were transferred to 96-well plates with cut bottoms. Seedlings were grown on water with a 16 h (light, 30°C)/8 h (dark, 26°C) rhythm for the indicated number of days. This condition was defined as the normal condition in our study.

For root architecture observation, dry seeds were dehulled and surface sterilized using 75% ethanol and sodium hypochlorite solution, and then planted on 1/2 MS medium in test tubes. The seedlings were grown for about 2 weeks with 16 h (light, 30°C)/8 h (dark, 26°C) rhythm until the longest root just reached the bottom of the tube (about 5–7 cm). The seedlings were carefully pulled out and gently washed with water, then photographed with a digital camera or stereoscopic microscope (Leica M125).

For protoplast preparation, seeds of *OsABIL2-ox-4* were dehulled and surface sterilized using 75% ethanol and sodium hypochlorite solution, and then planted on 1/2 MS medium in phyta trays. Seedlings were grown on water under short days with a 8 h light, 30°C and 16 h dark, 26°C cycle for 10 d. The phyta trays were covered by one layer of gauze to reduce the light.

Generation of transgenic rice plants

For overexpression of *OsABIL2*, the cDNA of *Os05g51510.1* (the canonical version according to UniprotKB, http://www.uniprot.org/uniprot/Q6L4R7) was cloned into the binary vector *pCAMBIA1306* fused with a FLAG-tag at the C-terminus. For overexpression of *OsABIL1* (*Os01g40094*), the open reading frame within the full-length cDNA of *OsABIL1* (*AK242616.1*) was cloned into *pCAMBIA1306*. The constructs were then transformed into DJ via *Agrobacterium tumefaciens* strain *EHA105*. The primers used for cloning *OsABIL2* and *OsABIL1* are listed in **Supplementary Table S1**.

Rice protoplast preparation

Protoplast preparation was carried out as described before (Zhang et al. 2011). After transformation, the protoplasts were incubated in the dark at room temperature for 10 h, and treated without ABA (mock) or with 100 μM ABA for another 2 h before cell fractionation analysis.

Pre-harvest sprouting determination

All mature panicles from six individual plants were harvested in the field, and all normally filled grains were collected. The seeds were dehulled, and their embryo status was carefully checked to determine PHS. Data are given as means ± SD.

ABA and drought treatments

For cell fraction analysis, the 3-week-old *OsABIL2-ox-4* plants were transplanted to solution with or without 5 μM ABA for 24 h. The plants were frozen in liquid nitrogen and stored at −80°C for protein extraction.

For ABA-responsive gene analysis, the 3-week-old seedlings grown under normal conditions were cut into about 0.5 cm long pieces and submerged in 50 μM ABA solution with 0.1% Triton X-100. After shaking for 2 h at 30°C, the samples were frozen in liquid nitrogen and stored at −80°C for RNA extraction.

For root hair induction assays, 3-day-old seedlings grown under normal conditions were transferred to solutions with different concentrations of ABA. After 36 h, the 1.5 cm young crown root tips were fixed in FAA solution (ethanol : acetic acid : 37% formaldehyde : H_2O, 50 : 5 : 10 : 35, by vol.), and then photographed with a stereoscopic microscope (Leica M125).

For growth inhibition assays, the 3-day-old seedlings grown under normal conditions were put into 2 μM ABA solution for 15 d. The seedlings were photographed, and plant height was measured by ImageJ software.

For drought treatment, the germinated DJ/*OsABIL2-ox-4* seeds were planted in a nested cup-pair and grown for about 3 weeks in a greenhouse. The nested cup-pair contains an intact outer cup and a perforated inner cup. During this period, some seedlings were removed to ensure the rest of the seedlings were at the same density. Then the outer cup was removed to release the water and watering was withheld for 3 weeks. At the re-watering stage, regular watering was resumed. Photographs were taken after new shoot sprouting.

Seed germination assays

Dry seeds were dehulled and surface sterilized using 75% ethanol and sodium hypochlorite solution. The sterilized seeds were planted on 1/2 MS medium with or without 1 μM ABA. The germination rate was counted each day for five consecutive days. Seeds with a visible coleoptile were counted as germinated seeds. The PHS seeds of the *OsABIL2-ox* lines were excluded in advance.

Water loss rate assays

Six leaves (the third leaf from the bottom) of the 3-week-old seedlings were cut and used, and three replicates were conducted. The leaves were put on weighing paper to allow natural drying (at a relative humidity of 45% and 30°C). The weight was recorded for 530 min with the indicated intervals.

SEM observation

Leaves of the 3-week-old seedlings were cut into 2 mm lengths and frozen in liquid nitrogen. The samples were thawed in FAA solution overnight. The fixed samples were gradient dehydrated in 50, 60, 70, 80, 90 and 100% ethanol for 1 h each, and then treated with solutions containing ethanol : *tert*-butyl alcohol (v/v), 3 : 1, 1 : 1 and 1 : 3, for 1 h each. Finally the samples were kept in pure *tert*-butyl alcohol. After vacuum freeze-drying, the samples were sputter-coated with Au–Pd and further visualized by SEM (Hitachi TM3000). For calculating the number of stomata, we counted all the stomata in 10 visual fields for each leaf fragment from three leaves. The stomatal density was determined as the stomatal number per square micron.

Cell fraction analysis

The cell fractionation analysis was carried out as described with slight modifications. (Wang et al. 2011). Rice samples were ground to a very fine powder in liquid nitrogen and lysed with fractionation buffer (20 mM Tris–HCl pH 7.0, 250 mM sucrose, 25% glycerol, 20 mM KCl, 2 mM EDTA, 2.5 mM $MgCl_2$, 30 mM β-mercaptoethanol, 1 × protease inhibitor cocktail and 0.7% Triton X-100). The obtained solution was filtrated (BD Falcon, 100 μM cell strainer) to remove tissue debris, and then the total filtrate with the resuspended deposit was centrifuged at 3,000 × *g* for 5 min. The resultant supernatant was filtrated with a 0.22 μm pore size filter membrane and used as the cytosolic fraction. The pellet was further washed with re-suspension buffer (20 mM Tris–HCl pH 7.0, 20 mM KCl, 2 mM EDTA, 2.5 mM $MgCl_2$, 30 mM β-mercaptoethanol, 1 × protease inhibitor cocktail) until the pellet was no longer green, and the the white pellet was resuspended to obtain the nuclear fraction. The protoplasts were harvested (150 × *g* for 5 min) and further suspended using fractionation buffer. After incubation on ice for 30 min, the cell fraction separation was conducted in the same way as for the samples from tissues ground in liquid nitrogen. Targets were detected by anti-FLAG antibody (Sigma) through Western blotting. The bands intensities were analyzed by Image J.

Yeast two-hybrid assay

The yeast two-hybrid assay was carried out as described previously (Y. Wang et al. 2013). OsABIL2 was constructed into pEXAD502, and OsPYL1 was constructed into pDBLeu.

Tobacco transient expression, BiFC assays and subcellular localization analysis

For subcellular localization analysis, the *OsABIL1* and *OsABIL2* fragments were inserted into a binary vector *pCAMBIA1300-mc* fused with *mCherry* at the C-terminus. The *OsPYL1* and the *SAPK10/8* cDNAs were constructed into the binary vector *pCAMBIA2302* fused with *GFP* at the C-terminus. For BiFC, the *OsABIL2* cDNA was constructed into *pXY104* fused with *YFP-C* at the C-terminus, and the *OsPYL1*, *SAPK8* and *SAPK10* were constructed into pXY106 fused with *YFP-N* at the N-terminus. The primers used for cloning *OsABIL2*, *OsPYL1*, *SAPK8* and *SAPK10* are listed in **Supplementary Table S1**. The tobacco transformations were carried out as previously described (Y. Wang et al. 2013).

In vitro pull-down assay and semi-in vivo pull-down assay

To obtain OsABIL2-His recombinant protein, the *OsABIL2* CDS (coding sequence) was inserted into pET-28a with 6 × His tags at both the N- and C-terminus. For maltose-binding protein (MBP)–OsPYL1 recombinant protein, the *OsPYL1* cDNA was cloned into the vector pMAL-c2x. For glutathione *S*-transferase (GST)–SAPK8, GST–SAPK10 and GST–OsABIL2 recombinant proteins, their cDNAs were each cloned into pGEX-4T-1. The primers used for cloning *OsABIL2*, *OsPYL1*, *SAPK10* and *SAPK8* are listed in **Supplementary Table S1**. The in vitro pull-down and semi-in vivo pull-down assays were carried out as described previously (Wang et al. 2011, Cai et al. 2014). Antibodies were from Santa Cruz (anti-GST), New East Biosciences (anti-His-tag) and Sigma (anti-FLAG), and polyclonal anti-MBP was produced in our lab by immunizing rabbits with full-length MBP protein.

For semi-in vivo competition assay, bead-bound bait was incubated with/without MBP–OsPYL1 and/or ABA (250 μM) in the rice total protein extract, and, for the samples with ABA treatment, the same concentration of ABA was added to the washing buffer.

For in vitro competition assay, His spintrap (GE Healthcare) was used to pull-down His-taged OsABIL2 in *Escherichia coli* lysate. Prey protein (GST–SAPK10) and *E. coli* lysate carrying OsABIL2-His was added into the binding buffer, and divided equally into seven parts. MBP–OsPYL1 (competitor), MBP (control) or ABA (250 μM) were directly added to the binding buffer, and the pull-down assay was carried out as for the His-tag protein purification protocol. For the samples with ABA treatment, the same concentration of ABA (250 μM) was added to the washing buffer.

Detection of phosphorylated protein by Phos-Tag marked SDS–PAGE

The proteins were incubated in dephosphorylation buffer [100 mM NaCl, 50 mM Tris–HCl, 10 mM $MgCl_2$, 1 mM dithiothreitol (DTT), pH 7.5] for 1.5 h at 37°C. The reaction samples were divided and separated by SDS–PAGE (8%) or SDS–PAGE (8%) containing 25 μM Phos-Tag with 100 μM $MnCl_2$. The bands were visualized by Coomassie Brilliant Blue (CBB) staining.

Quantitative real-time PCR assays

The qRT-PCR assays were carried out as described previously with slight modifications (Zhang et al. 2009). The primers for qRT-PCR were designed by Beacon design 8.0 software to avoid the homolog regions, shown in **Supplementay Table S1**. The RNAs were extracted using aPlant RNAprep Kit (Tiangen). About 3 μg of total RNA was used for reverse transcription (M-MLV reverse trascriptase, TAKARA). The RT-PCRs were carried out with a Mastercycler $Realplex_2$ system (Eppendorf), and PCR products were monitored by SYBR green dye. The expression level was normalized by the expression of *OsACTIN1* (internal control), and the fold changes were analyzed via the $2^{-\Delta\Delta CT}$ method.

Phylogenetic analysis

The sequences of Arabidopsis genes were obtained from TAIR (http://www.Arabidopsis.org/); and the sequences of rice genes were obtained from RGAP (http://rice.plantbiology.msu.edu/index.shtml). The multiple sequence alignments were performed with Clustal Omega (http://www.ebi.ac.uk/Tools/msa/clustalo/) using default parameters. The phylogenetic trees were constructed using MEGA (version 5.22) through the Neighbor–Joining method. Bootstrap analysis was performed with 1,000 replicates, and the bootstrap values are shown at the nodes.

Supplementary data

Supplementary data are available at PCP online.

Funding

This work was supported by the National Natural Science Foundation of China [grant No. 91317302 (to X.W.)]; the National Basic Research Program of China [grant No. 2012CB114300 (to X.W.)].

Disclosures

The authors have no conflicts of interest to declare.

Acknowledgements

We thank Professor Gynheung An for providing the rice T-DNA lines, and our colleagues Mengran Yang, Jianjun Jang, Zhenying Cai and Professor Wei Su of Fudan University and Zhongming Fang of Huazhong Agricultural University for proofreading the text.

References

Antoni, R., Gonzalez-Guzman, M., Rodriguez, L., Peirats-Llobet, M., Pizzio, G.A., Fernandez, M.A., et al. (2013) PYRABACTIN RESISTANCE1-LIKE8 plays an important role for the regulation of abscisic acid signaling in root. *Plant Physiol.* 161: 931–941.

Cai, Z., Liu, J., Wang, H., Yang, C., Chen, Y., Li, Y., et al. (2014) GSK3-like kinases positively modulate abscisic acid signaling through phosphorylating subgroup III SnRK2s in *Arabidopsis*. *Proc. Natl. Acad. Sci. USA* 111: 9651–9656.

Chae, M.J., Lee, J.S., Nam, M.H., Cho, K., Hong, J.Y., Yi, A.A., et al. (2007) A rice dehydration-inducible SNF1-related protein kinase 2 phosphorylates an abscisic acid responsive element-binding factor and associates with ABA signaling. *Plant Mol. Biol.* 63: 151–169.

Chen, C.W., Yang, Y.W., Lur, H.S., Tsai, Y.G. and Chang, M.C. (2006) A novel function of abscisic acid in the regulation of rice (*Oryza sativa* L.) root growth and development. *Plant Cell Physiol.* 47: 1–13.

Choi, H.I., Hong, J.H., Ha, J.K., Kang, J.Y. and Kim, S.Y. (2000) ABFs, a family of ABA-responsive element binding factors. *J. Biol. Chem.* 275: 1723–1730.

Duan, L., Dietrich, D., Ng, C.H., Chan, P.M., Bhalerao, R., Bennett, M.J., et al. (2013) Endodermal ABA signaling promotes lateral root quiescence during salt stress in *Arabidopsis* seedlings. *Plant Cell* 25: 324–341.

Fujii, H., Chinnusamy, V., Rodrigues, A., Rubio, S., Antoni, R., Park, S.Y., et al. (2009) In vitro reconstitution of an abscisic acid signalling pathway. *Nature* 462: 660–664.

Fujii, H., Verslues, P.E. and Zhu, J.K. (2007) Identification of two protein kinases required for abscisic acid regulation of seed germination, root growth, and gene expression in *Arabidopsis*. *Plant Cell* 19: 485–494.

Fujii, H., Verslues, P.E. and Zhu, J.K. (2011) *Arabidopsis* decuple mutant reveals the importance of SnRK2 kinases in osmotic stress responses in vivo. *Proc. Natl. Acad. Sci. USA* 108: 1717–1722.

Fujii, H. and Zhu, J.-K. (2009) *Arabidopsis* mutant deficient in 3 abscisic acid-activated protein kinases reveals critical roles in growth, reproduction, and stress. *Proc. Natl. Acad. Sci. USA* 106: 8380–8385.

Fujita, Y., Nakashima, K., Yoshida, T., Katagiri, T., Kidokoro, S., Kanamori, N., et al. (2009) Three SnRK2 protein kinases are the main positive regulators of abscisic acid signaling in response to water stress in Arabidopsis. *Plant Cell Physiol.* 50: 2123–2132.

Geng, Y., Wu, R., Wee, C.W., Xie, F., Wei, X., Chan, P.M.Y., et al. (2013) A spatio-temporal understanding of growth regulation during the salt stress response in *Arabidopsis*. *Plant Cell* 25: 2132–2154.

He, Y., Hao, Q., Li, W., Yan, C., Yan, N. and Yin, P. (2014) Identification and characterization of ABA receptors in *Oryza sativa*. *PLoS One* 9: e95246.

Jeon, J.S., Lee, S., Jung, K.H., Jun, S.H., Jeon, D.H., Lee, J., et al. (2000) T-DNA insertional mutagenesis for functional genomics in rice. *Plant J.* 22: 561–570.

Jeong, D.H., An, S., Park, S., Kang, H.G., Park, G.G., Kim, S.R., et al. (2006) Generation of a flanking sequence-tag database for activation-tagging lines in japonica rice. *Plant J.* 45: 123–132.

Kagaya, Y., Hobo, T., Murata, M., Ban, A. and Hattori, T. (2002) Abscisic acid-induced transcription is mediated by phosphorylation of an abscisic acid response element binding factor, TRAB1. *Plant Cell* 14: 3177–3189.

Kang, J.-y., Choi, H.-i., Im, M.-y. and Kim, S.Y. (2002) *Arabidopsis* basic leucine zipper proteins that mediate stress-responsive abscisic acid signaling. *Plant Cell* 14: 343–357.

Kim, H., Hwang, H., Hong, J.W., Lee, Y.N., Ahn, I.P., Yoon, I.S., et al. (2012) A rice orthologue of the ABA receptor, OsPYL/RCAR5, is a positive regulator of the ABA signal transduction pathway in seed germination and early seedling growth. *J. Exp. Bot.* 63: 1013–1024.

Kobayashi, Y., Murata, M., Minami, H., Yamamoto, S., Kagaya, Y., Hobo, T., et al. (2005) Abscisic acid-activated SNRK2 protein kinases function in the gene-regulation pathway of ABA signal transduction by phosphorylating ABA response element-binding factors. *Plant J.* 44: 939–949.

Kobayashi, Y., Yamamoto, S., Minami, H., Kagaya, Y. and Hattori, T. (2004) Differential activation of the rice sucrose nonfermenting1-related protein kinase2 family by hyperosmotic stress and abscisic acid. *Plant Cell* 16: 1163–1177.

Leung, J., Bouvier-Durand, M., Morris, P.C., Guerrier, D., Chefdor, F. and Giraudat, J. (1994) *Arabidopsis* ABA response gene *ABI1*: features of a calcium-modulated protein phosphatase. *Science* 264: 1448–1452.

Leung, J., Merlot, S. and Giraudat, J. (1997) The *Arabidopsis ABSCISIC ACID-INSENSITIVE2* (*ABI2*) and *ABI1* genes encode homologous protein phosphatase 2C involed in abscisic asid signal transduction. *Plant Cell* 9: 759–771.

Li, Y.S., Sun, H., Wang, Z.F., Duan, M., Huang, S.D., Yang, J., et al. (2013) A novel nuclear protein phosphatase 2C negatively regulated by ABL1 is involved in abiotic stress and panicle development in rice. *Mol. Biotechnol.* 54: 703–710.

Ma, Y., Szostkiewicz, I., Korte, A., Moes, D., Yang, Y., Christmann, A., et al. (2009) Regulators of PP2C phosphatase activity function as abscisic acid sensors. *Science* 324: 1064–1068.

Merlot, S., Gosti, F., Guerrier, D., Vavasseur, A. and Giraudat, J. (2001) The ABI1 and ABI2 protein phosphatases 2C act in a negative feedback regulatory loop of the abscisic acid signalling pathway. *Plant J.* 25: 295–303.

Meyer, K., Leube, M.P. and Grill, E. (1994) A protein phosphatase 2C involved in ABA signal transduction in *Arabidopsis thaliana*. *Science* 264: 1462–1455.

Mickelbart, M.V., Hasegawa, P.M. and Bailey-Serres, J. (2015) Genetic mechanisms of abiotic stress tolerance that translate to crop yield stability. *Nat. Rev. Genet.* 16: 237–251.

Moes, D., Himmelbach, A., Korte, A., Haberer, G. and Grill, E. (2008) Nuclear localization of the mutant protein phosphatase abi1 is required for insensitivity towards ABA responses in *Arabidopsis*. *Plant J.* 54: 806–819.

Mustilli, A.C., Merlot, S., Vavasseur, A., Fenzi, F. and Giraudat, J. (2002) *Arabidopsis* OST1 protein kinase mediates the regulation of stomatal aperture by abscisic acid and acts upstream of reactive oxygen species production. *Plant Cell* 14: 3089–3099.

Nishimura, N., Sarkeshik, A., Nito, K., Park, S.-Y., Wang, A., Carvalho, P.C., et al. (2009) PYR/PYL/RCAR family members are major in-vivo ABI1 protein phosphatase 2C-interacting proteins in *Arabidopsis*. *Plant J.* 61: 290–299.

Park, S.Y., Fung, P., Nishimura, N., Jensen, D.R., Fujii, H., Zhao, Y., et al. (2009) Abscisic acid inhibits type 2C protein phosphatases via the PYR/PYL family of START proteins. *Science* 324: 1068–1071.

Rubio, S., Rodrigues, A., Saez, A., Dizon, M.B., Galle, A., Kim, T.-H., et al. (2009) Triple loss of function of protein phosphatases type 2C leads to partial constitutive response to endogenous abscisic acid. *Plant Physiol.* 150: 1345–1355.

Saab, I.N., Sharp, R.E., Pritchard, J. and Voetberg, G.S. (1990) Increased endogenous abscisic acid maintains primary root growth and inhibits shoot growth of maize seedlings at low water potentials. *Plant Physiol.* 93: 1329–1336.

Saez, A., Robert, N., Maktabi, M.H., Schroeder, J.I., Serrano, R. and Rodriguez, P.L. (2006) Enhancement of abscisic acid sensitivity and reduction of water consumption in *Arabidopsis* by combined inactivation of the protein phosphatases type 2C ABI1 and HAB1. *Plant physiol.* 141: 1389–1399.

Shinozaki, K. and Yamaguchi-Shinozaki, K. (2007) Gene networks involved in drought stress response and tolerance. *J. Exp. Bot.* 58: 221–227.

Singh, A., Jha, S.K., Bagri, J. and Pandey, G.K. (2015) ABA inducible rice protein phosphatase 2C confers ABA insensitivity and abiotic stress tolerance in *Arabidopsis*. *PLoS One* 10: e0125168.

Tanaka, Y., Nose, T., Jikumaru, Y. and Kamiya, Y. (2013) ABA inhibits entry into stomatal-lineage development in Arabidopsis leaves. *Plant J.* 74: 448–457.

Todaka, D., Nakashima, K., Shinozaki, K. and Yamaguchi-Shinozaki, K. (2012) Toward understanding transcriptional regulatory networks in abiotic stress responses and tolerance in rice. *Rice* 5: 1–9.

Umezawa, T., Sugiyama, N., Mizoguchi, M., Hayashi, S., Myouga, F., Yamaguchi-Shinozaki, K., et al. (2009) Type 2C protein phosphatases directly regulate abscisic acid-activated protein kinases in *Arabidopsis*. *Proc. Natl. Acad. Sci. USA* 106: 17588–17593.

Wang, H., Yang, C., Zhang, C., Wang, N., Lu, D., Wang, J., et al. (2011) Dual role of BKI1 and 14-3-3s in brassinosteroid signaling to link receptor with transcription factors. *Dev. Cell* 21: 825–834.

Wang, P., Xue, L., Batelli, G., Lee, S., Hou, Y.-J., Van Oosten, M.J., et al. (2013) Quantitative phosphoproteomics identifies SnRK2 protein kinase substrates and reveals the effectors of abscisic acid action. *Proc. Natl. Acad. Sci. USA* 110: 11205–11210.

Wang, Y., Sun, S., Zhu, W., Jia, K., Yang, H. and Wang, X. (2013) Strigolactone/MAX2-induced degradation of brassinosteroid transcriptional effector BES1 regulates shoot branching. *Dev. Cell* 27: 681–688.

Xu, W., Jia, L., Shi, W., Liang, J., Zhou, F., Li, Q., et al. (2013) Abscisic acid accumulation modulates auxin transport in the root tip to enhance proton secretion for maintaining root growth under moderate water stress. *New Phytol.* 197: 139–150.

Zhang, S., Cai, Z. and Wang, X. (2009) The primary signaling outputs of brassinosteroids are regulated by abscisic acid signaling. *Proc. Natl. Acad. Sci. USA* 106: 4543–4548.

Zhang, Y., Su, J., Duan, S., Ao, Y., Dai, J., Liu, J., et al. (2011) A highly efficient rice green tissue protoplast system for transient gene expression and studying light/chloroplast-related processes. *Plant Methods* 7: 30.